Coke Formation in Steam Cracking Reactors: Deciphering the Impact of Aromatic Compounds and Temperature on Fouling Dynamics

Hamed Mohamadzadeh Shirazi[1], *Lucas dos Santos Vargette*[1], *Georgios Bellos*[2], *Yannick Ureel*[1], *Melissa N. Dunkle*[2], *Steven Corthals*[2], *Marie-Françoise Reyniers*[1], *Kevin M. Van Geem*[1,*]

[1]Laboratory for Chemical Technology, Ghent University, Technologiepark 121, B-9052 Gent, Belgium

[2]Dow Benelux B.V., Dowweg 5, 4542NM Hoek, The Netherlands

[*] Corresponding author: Technologiepark 125, B-9052 Zwijnaarde, Belgium;

Kevin.VanGeem@UGent.be

KEYWORDS: Steam Cracking; Olefin; Coke Formation; Fouling Mechanism; Aromatics; Temperature

Abstract:

Formation of coke poses a considerable challenge in steam cracking reactors utilized for olefin production, exerting detrimental effects on reactor performance and productivity. To tackle this challenge, a more profound understanding of fouling phenomena and their intricate connections with feedstock composition and process conditions is imperative. While conventional wisdom suggests that all aromatics contribute to increased coke formation, our research challenges this assumption. To evaluate this assumption an investigation was conducted to measure the coking tendency of single-ring aromatics, double-ring aromatics, and naphtheno-diaromatic compounds by introducing them to a naphtha sample. On one hand, the incorporation of single-ring aromatics, up to 9 wt.%, resulted in a 12% reduction in the overall coke formation rate across the radiant and TLE sections. Conversely, the introduction of 2 wt.% double-ring aromatics exhibited a marginal 4% increase in coking rates. However, the introduction of a naphtheno-diaromatic compound led to a 35% increase in coke formation rates in the radiant and TLE sections. On the other hand, temperature emerged as a more significant factor influencing coke formation within steam cracking reactions. Elevating the coil outlet temperature (COT) from 950 °C to 970 °C resulted in a minimum 40% rise in the asymptotic coking rates. This study underscores the importance of comprehending coke formation mechanisms in steam cracking reactors and developing effective methods to mitigate fouling.

1. Introduction

Steam cracking is a vital industrial process for the production of light olefins. However, this process generates aromatic, naphtheno-aromatic, and olefinic products that contribute to coke deposition on the inner walls of cracker furnaces [1-4]. The accumulation of these coke-like deposits in the pyrolysis reactor and transfer line exchanger (TLE) frequently necessitates industrial unit shutdowns and adversely impacts process economics [5-7].

Extensive research has been conducted to comprehend the mechanisms of coke formation using both theoretical [8, 9] and experimental [5, 10-12] approaches. Previous studies have proposed three mechanisms: catalytic heterogeneous, non-catalytic heterogeneous, and non-catalytic homogeneous [12]. The catalytic heterogeneous mechanism primarily occurs in the early stages of cracking, where the catalytic sites on the reactor material remain bare without a coke layer [7]. Conversely, the non-catalytic stage in the radiant section heavily depends on feedstock properties. It involves the gradual encapsulation of the material surface with carbonaceous coke, resulting from the reaction between gas-phase coke precursors and partially dehydrogenated filaments on the tube surface [13]. Over time, this mechanism becomes increasingly dominant as the available catalytic sites become covered by coke [14-16]. The third mechanism, which is entirely dependent on feedstock properties, involves the condensation of high boiling point components in the product, leading to the accumulation of polyaromatic hydrocarbons (PAHs). These PAHs serve as primary structural components of coke in lower temperature sections, such as the TLE [9, 13, 17, 18]. Consequently, a higher presence of pyrolysis fuel oil (PFO, C_{10+}) in the reactor effluent leads to increased fouling in the TLE section of a steam cracker.

Hence, considering both the non-catalytic heterogeneous and non-catalytic homogeneous mechanisms, it becomes essential to comprehend how the composition of the feedstock and the conditions of the reaction impact the coke precursors, and subsequently, the coking rate. For instance, naphtha crackers typically require shutdowns after 60-80 days due to excessively high tube metal temperatures caused by the buildup of coke, while ethane furnaces have longer operation times [19]. Process conditions, particularly temperature, significantly influence coke formation or fouling on the inner wall of reactors by facilitating the formation of coke by-products through secondary reactions and reducing the furnace's operational duration. Gál and Lakatos [20] conducted a study to examine the influence of coil outlet temperature (COT) on product yield and coke formation rate during steam cracking using natural gas as the feedstock. Their findings revealed that increasing the COT from 830°C to 845°C resulted in an increase in ethylene yield from 30 wt.% to 35 wt.%. However, subsequent temperature increments up to 850°C did not notably further enhance the yield; instead, a significant increase in the production of coke occurred, going from 7×10^{-3} wt.% to 23×10^{-3} wt.% when the temperature rose from 830°C to 850°C.

The feedstock utilized in steam cracking is typically a mixture of hydrocarbons with varying compositions based on the source and processing method. Obtaining reliable information regarding the individual contributions of hydrocarbons as constituents of complex steam cracker feedstocks to coke formation is of utmost importance. While previous literature, including the works of Kopinke et al. [5, 21, 22], has partially explored these phenomena, recent reviews highlight the necessity for a better understanding of the relationship between hydrocarbon structure, particularly the presence of aromatics, and their propensity to form carbonaceous deposits [9, 13, 17, 23, 24].

Aromatics are widely believed to have a high tendency to form coke due to their similarity with the mostly aromatic coking layer [22, 24-26]. To validate this hypothesis, the current study delves into the impact of aromatics on coke formation. This research not only questions the dominant notion that aromatics are the leading contributors to coke generation in steam cracking reactors but also seeks to substantiate this theory. To achieve this, various steam cracking and coke measurement experiments were designed and conducted using reference naphtha spiked with varying percentages of single-ring aromatics, a double-ring aromatic, and a naphtheno-diaromatic compounds. To our knowledge, this is the first instance where the coking tendency measurements of aromatics have been tested using a well-defined reference feedstock composition, carried out in a bench-scale setup that emulates the radiant and TLE sections of an authentic industrial cracker. In the current study, which focuses on investigating the influence of feedstock on coking, a total of six samples were tested, each test being repeated. These samples include reference naphtha (RN), reference naphtha with 3wt.% single-ring aromatics (A1), 6wt.% single-ring aromatics (A2), and 9wt.% single-ring aromatics (A3), as well as 2wt.% double-ring aromatics (AA) and 1.2wt.% naphtheno-diaromatic (NAA).

In addition to investigating the impact of feedstock composition on coke formation, a series of experiments were conducted to examine how temperature influences the formation of coke, as well as to investigate the relative effects of temperature and feedstock composition on coke formation and fouling. To explore these factors, four separate experimental sets were executed using two different feedstocks: A1 and NAA samples. These feedstocks underwent a cracking temperature increase of 20°C in the radiant section, as compared to the conditions employed in the feedstock effect tests.

For these purposes, the study utilized the Fouling Assessment SeTup (FAST), a bench-scale steam cracker, which allows for the assessment of fouling in the radiant and transfer line exchanger (TLE) sections within a single experimental run using two methods: offline, by burning coke and detecting the produced CO/CO_2 with IR, and online, by using a coupon hung inside the reactor and measuring the increased weight of coke deposits over time using a magnetic suspension balance (MSB). The latter method allowed the calculation of the catalytic and asymptotic coking rates.

2. Materials and Methods

2.1. Fouling Assessment SeTup (FAST)

The unit has been thoroughly described in a previous publication by Geerts et al. [3]. However, modifications specifically relevant to this work are summarized here. The FAST (Fouling Assessment SeTup) is an experimental apparatus designed to evaluate the tendency for fouling in steam cracking reactions across a wide range of feedstocks e.g., naphtha, gas condensates, and pyrolysis oil [3]. The unit comprises multiple sections, including feed, convection, reaction, and analysis sections, as illustrated in the simplified schematic in Figure 1. A Programmable Logical Controller (PLC) is utilized to maintain control over various process parameters.

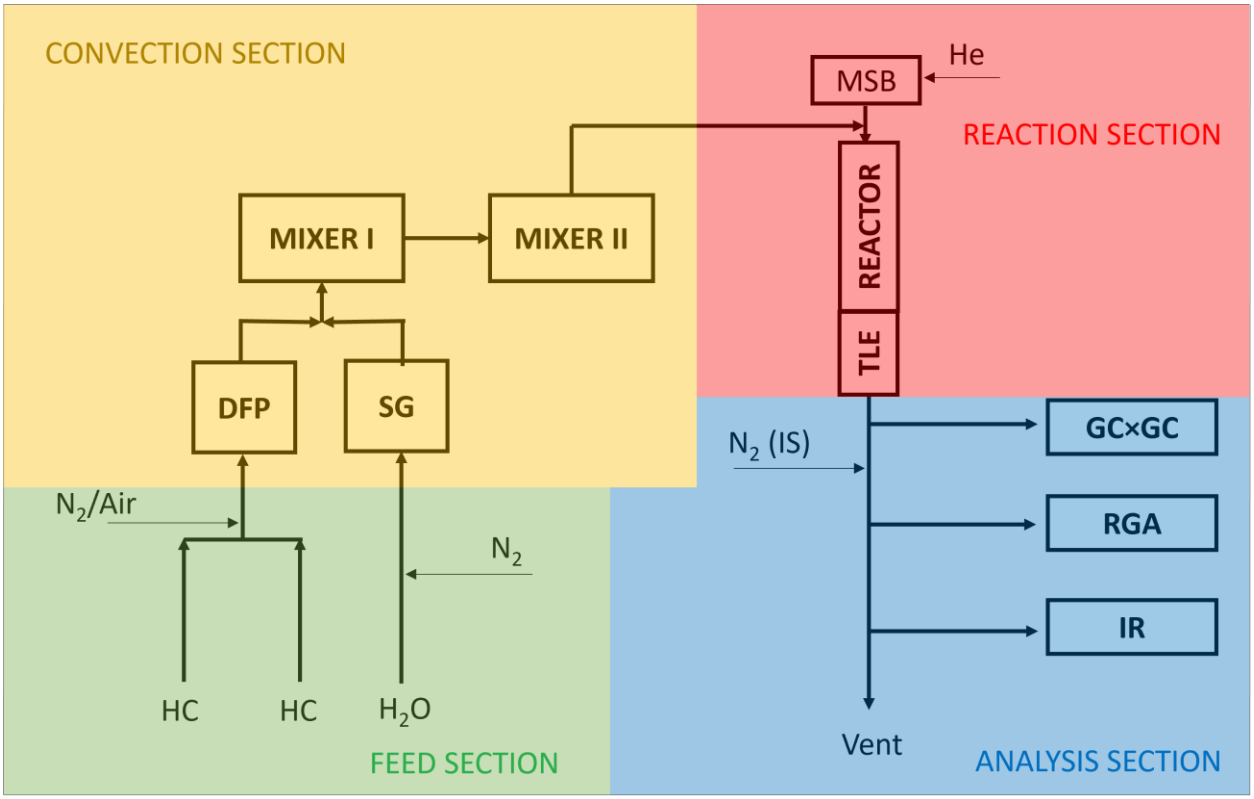

Figure 1. Simplified schematic of the Fouling Assessment SeTup (FAST). DFP: dry feed preheater, SG: steam generator, MSB: magnetic suspension balance, RGA: refinery gas analyzer, GC×GC: 2-D gas chromatography.

2.1.1. Feed section

In the feed section, the mass flow rates of liquids, hydrocarbon (HC) and water, are controlled via Coriolis mass flow controllers (Bronkhorst, the Netherlands) in conjunction with high-precision rotary pumps (HNP, Germany). For regulating gaseous feeds of helium, nitrogen, and air, the same mass flow meter is utilized along with regulating valves (HNP, Germany). To ensure an adequate suction pressure for the pumps, the hydrocarbon and water vessels are pressurized with nitrogen. The possibility of pump blockage due to solid impurities is prevented by employing sintered filters (10 µm) located in two parallel cartridges upstream of the pumps. This arrangement allows the hydrocarbon feed to be redirected to the second filter in case the first one becomes blocked. The homogeneity of the hydrocarbon feed is ensured by employing electrical heating and continuous

agitation through electrical impellers inside the feed container. To prevent condensation of the hydrocarbon and the occurrence of phase separation, the lines in the feeding section are heated by tracing. Nitrogen, serving as the primary internal standard, is injected into the downstream part of the TLE for determining the effluent yields [27, 28]. To safeguard the interior parts of the MSB from direct contact with the hot gases exiting the convection section, a flow of helium is used to purge the MSB cage [10].

2.1.2. Convection section

The convection section comprises three distinct zones: the Dry Feed Preheater (DFP), Mixer I, and Mixer II. All heating elements consist of vertically positioned electrically heated Incoloy 600 tubes. These tubes are housed within a three-section electrically heated insulation box, which serves the purpose of reducing heat loss to the surrounding environment and preventing the formation of cold spots. To monitor the temperature of each element, a regulating K-type thermocouple is positioned on the outer wall of the heating element outlet. The DFP and Steam Generator (SG) are filled with quartz beads to facilitate smooth evaporation, while Mixer I and Mixer II incorporate internal static mixers to ensure uniform blending of the hydrocarbon and steam diluent. The hydrocarbon and water enter the DFP and SG, respectively, and they converge upstream of the series of mixers. The output of the convection section is transferred to the reactor via a High Temperature Transferline (HTTL), which serves a similar purpose as the Crossover Temperature (XOT) in industrial steam crackers.

2.1.3. Reaction section

The homogenous vaporized mixture of hydrocarbon and steam which is the outlet of the convection section is fed from the top side of the Incoloy 800HT reactor (33/21 Cr-Ni) with 0.6 m length and 10 mm internal diameter. The reactor divides into four zones, 0.15 m long each (Figure

2). The first three zones are the radiant parts where steam cracking occurs and their outer walls temperatures are controlled with an electrically heated furnace, while the last part is the TLE and the related temperature is controlled by the electrically heated furnace in combination with the injection of air through a spiral wrapped around the coil. Therefore, the temperature setting at this part of the reactor is attained by adjusting simultaneously the input heat from the furnace and the flow rate of cooling air.

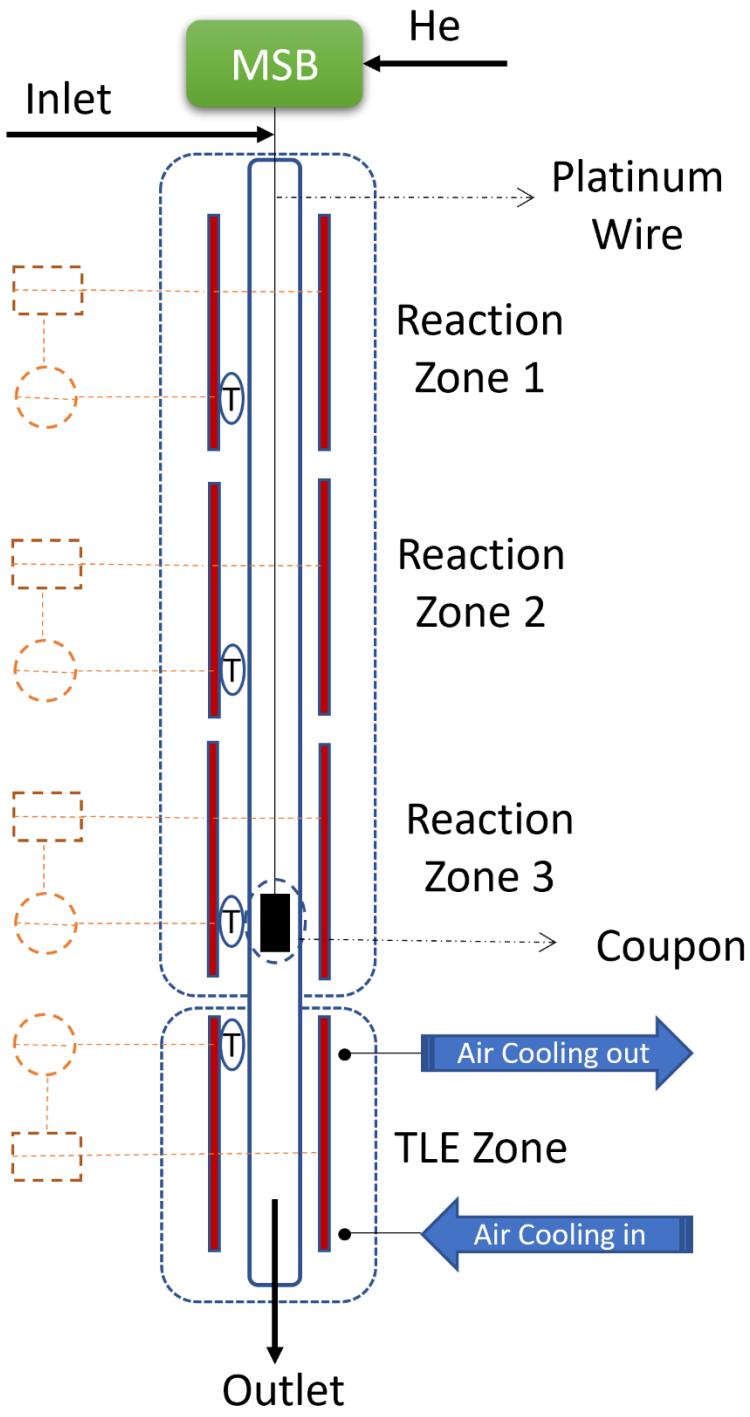

Figure 2. Four zones within the reactor section and the location of the suspended coupon within the radiant section.

As mentioned in Section 1, the measurement of deposited coke mass is conducted through two methods: online and offline. For online measurement, a coupon (10×4×1 mm) (35/45 Cr-Ni) is

suspended in Reaction Zone 3 of the reactor (0.38 m from the reactor inlet) using a Platinum wire (diameter 0.5 mm) hung from the MSB (Linseis Thermal Analysis). Online coke measurement for the TLE section is also possible by increasing the length of the Platinum wire, which is not the purpose of this study (see Figure 2). The MSB continuously measures the added mass of coke, resulting from fouling on the flat coupon, over time with a resolution of ± 5 µg at a frequency of 1 Hz. To ensure accurate measurements, controlling pressure is crucial due to its impact on MSB performance. To address this, pressure is controlled during each run using a Back Pressure Regulator (BPR) positioned downstream of the reaction section. Moreover, the pressure drop increase caused by coke formation inside the reactor tube is monitored by pressure transmitters installed at the reactor's inlet and outlet. The advantage of this method lies in the calculation of initial (catalytic) and asymptotic coking rates. The data obtained from the MSB measurements contains high-frequency noise, which is filtered using a MATLAB 8.6 2015b (The Mathworks, Inc.) low-pass filter. The coke mass curve is then regressed using Eq. (1), where m_t represents the coke mass on the coupon's surface at time t, A is the asymptotic coking rate contribution, B is the overall importance of the catalytic coking rate contribution, C is the catalytic coking rate contribution (e.g., Ni), and D is the catalytic coking rate contribution (e.g., Fe). Eq. (1) describes the phenomenological behavior of coke formation rather than relying on a theoretical model. Detailed information on the calculation of the coking rate using online coke measurement can be found in section S1 of the Supporting Information.

$$m_t = At + B\left(1 - \frac{1}{2}(e^{-Ct} + e^{-Dt})\right) \qquad \text{Eq. (1)}$$

By taking the derivative of Eq. (1) with respect to time, the corresponding rate of mass increase can be determined using Eq. (2), where r_c represents the coking rate.

$$r_c = \frac{dm_t}{dt} = A + \frac{B}{2}(Ce^{-Ct} + De^{-Dt}) \quad \text{Eq. (2)}$$

Finally, dividing the coking rate r_c by the coupon's surface area yields the coking rate equation on the coupon's surface, as shown in Eq. (3).

$$r_f = \frac{r_c}{S_c} \quad \text{Eq. (3)}$$

Regarding the offline measurement, the carbonaceous fouling deposits are burned off with air/steam after the cracking experiment, and the CO/CO_2 products are detected using IR spectroscopy. The amount of produced gases is then correlated with the mass of formed coke. It is worth noting that the first three zones of the reactor are decoked after the TLE part, as burning the coke deposits on the TLE during radiant decoking would occur otherwise. For more information on the detailed decoking procedure, including temperature profiles and flow rates, please refer to section S4 in the Supporting Information. While the deposited coke on the coupon is burned off during reactor decoking, it does not affect the decoking results since the surface area of the coupon is negligible compared to that of the reactor. Consequently, unlike the online method, the fouling rate represents the average coke formation during the duration of the experiment.

2.1.4. Analysis section

The analysis section of the setup performs online compositional analysis of a broad range of products with varying boiling points, including N_2, H_2, CO, CO_2, and hydrocarbons spanning from methane to polycyclic aromatic hydrocarbons (PAHs). A fraction of the effluent, consisting of N_2, H_2, CO, CO_2, and low-boiling hydrocarbons (C_1-C_4), is separated chromatographically and detected by a Refinery Gas Analyzer (RGA) equipped with two Thermal Conductivity Detectors (TCD) and one Flame Ionization Detector (FID). Additionally, comprehensive two-dimensional gas chromatography (GC×GC) coupled with an FID detector is utilized to detect all hydrocarbons

from methane to PAHs. The identification of major reaction products is determined through a chromatographic retention times database obtained by injecting standard mixtures or employing mass spectrometry identification. Minor products are identified using Kovats retention indices and the roof-tile principle [27, 29]. In both cases, the identification of components is based on the internal standard methodology [27-29]. section S3 of the Supporting Information provides a comprehensive description of the composition analysis procedure for samples, and the operating temperature programs for RGA and GC×GC.

As mentioned in section 2.1.3, the quantity of formed coke is measured through online and offline methods. In the offline method, inner wall coke in a specific section of the reactor is burned off using hot air/steam gases. After cooling the combustion gases to 20°C, the flow of the effluent is measured using a drum rotor volumetric gas meter (Ritter) at a controlled pressure of 120 kPa. Volumetric concentrations of CO and CO_2 are determined using an infrared analyzer (IR) from Fuji (Fuji Electric) with a frequency of 50 mHz, exploiting the absorption of specific infrared wavelengths by carbon oxides. To calibrate the IR cell for measuring light intensity, a bottle containing 15 vol.% CO_2 and 10 vol.% CO is used as the upper limit, while nitrogen is used to calibrate the zero intensity as a reference point. By employing the Lambert-Beer law, the quantification of carbon oxides is accurately calculated. Finally, using Eq. (4), the mass of coke is calculated as a cumulative value over the entire decoking period.

$$m_c = MM_c \sum_{i=0}^{N} \frac{\dot{Q}_t \times \left(y_{CO,i} + y_{CO_2,i}\right) \times p_i}{R \times (\mathrm{T} + 273)} \qquad \text{Eq. (4)}$$

In Eq. (4), MM_c represents the molecular mass of pure coke (12 g/mol), $\dot{Q}_t$ is the volumetric flow rate of decoking effluent (m^3/s), R is the gas constant ($J.mol^{-1}.K^{-1}$), y denotes the volumetric concentration of component CO/CO_2 at time i, p_i is the pressure (Pa) at time i, and T is the

temperature (°C). To determine the average fouling rates (mg/h), the mass of coke (m_c) is divided by the six-hour duration of the cracking run (t_c), as shown in Eq. (5).

$$R_c = \frac{m_c}{t_c} \times 10^3 \quad \text{Eq. (5)}$$

2.2. Feedstocks and Analytical Gases

For the preparation of solutions used in both presulfidation and continuous sulfidation processes, dimethyl disulfide (DMDS, Thermo Fisher Scientific, 99%) was employed. Furthermore, the study also made use of analytical gases — H_2, N_2, and He — with a minimum purity of 99.999. The selected feedstock sample is a conventional reference naphtha, and the GC×GC-FID chromatogram corresponding to this sample can be found in Figure S.2 of the Supporting Information. Furthermore, the detailed composition analysis (PIONA analysis) for the reference naphtha sample is presented in Table 1. The detailed GC×GC settings can be obtained in section S2 of the Supporting Information. The density of the naphtha at normal temperature and pressure conditions (NTP) is 667 $kg.m^{-3}$.

Table 1. PIONA composition analysis of the reference naphtha sample.

Carbon Number	n-Paraffin	Iso-paraffin	Olefin	Naphthene	Aromatic
4	0.41	0.02	0.00	0.00	0.00
5	10.89	15.08	0.00	1.56	0.00
6	10.05	18.44	0.00	12.81	0.63
7	5.25	9.10	0.00	12.02	0.85
8	0.17	2.25	0.00	0.46	0.00
Total	26.77	44.89	0.00	26.86	1.48

The reference naphtha sample was deliberately spiked with different weight percentages of aromatic compounds, as shown in Table 2. More specifically, the A1, A2, and A3 samples were

made by adding benzene (Sigma-Aldrich, ≥99.7%) and toluene (Sigma-Aldrich, 99.8%) to the reference naphtha resulting in final aromatic contents of 3 wt.%, 6 wt.%, and 9 wt.%, respectively. Additionally, the AA and NAA samples were prepared by adding 2 wt.% of naphthalene (Sigma-Aldrich, 99%) and 1.2 wt.% of acenaphthylene (TCI America™, >94%). The percentages of spiked single- and double-ring aromatics are carefully selected based on typical concentrations found in naphtha cracking products. The addition of more than 1.2 wt.% of acenaphthylene is not possible due to its limited solubility in naphtha.

Table 2. Aromatic composition analysis of prepared feedstock samples.

Compound (wt.%)	Feedstock					
	RN	A1	A2	A3	AA	NAA
Benzene	0.63	1.28	2.57	3.90	0.63	0.63
Toluene	0.85	1.72	3.43	5.10	0.85	0.85
Total Benzene+Toluene	1.48	3.00	6.00	9.00	1.48	1.48
Naphthalene	0.00	0.00	0.00	0.00	2.00	0.00
Acenaphthylene	0.00	0.00	0.00	0.00	0.00	1.20

2.3. Experimental conditions and procedure

Table 3 presents a summary of the experimental conditions employed in this study. Throughout all the experiment steps, a constant flow of helium at a rate of 5 g/h was maintained to the MSB cage. This precautionary measure aimed to safeguard the interior components from the high-temperature gases and prevent any potential contamination. Prior to each cracking experiment, a pretreatment process was conducted to create an oxide layer on the surfaces of the reactor and coupon. This pretreatment is essential before each run to facilitate the diffusion of coke-resistant

elements (such as Cr) from the bulk of the alloy to the surface, thereby enhancing the metal's resistance to coke formation [7, 10, 30]. Furthermore, a presulfidation step was performed for 30 minutes using a solution containing 500 wt. ppm of DMDS at a mass flow rate of 35 g/h. During this step, the temperature of Reaction Zone 3 was maintained at 827°C. The presulfidation process is believed to establish a protective sulfur layer just before the cracking reaction, reducing direct contact between the hydrocarbon gas phase and the metal surface during the initial stages of the reaction, where the catalytic mechanism prevails [31-33].

During the cracking phase, hydrocarbon with a flow rate of 140 g/h was supplied to the Dy Feed Preheater (DFP), while demineralized water containing 60 wt. ppm DMDS (7.13 wt. ppm S/HC) was fed to the Steam Generator (SG) at a flow rate of 49 g/h (resulting in a dilution of 0.35 g water/g HC). The steam generated in the SG was mixed with the hydrocarbon downstream of the DFP and upstream of Mixer I. To achieve the desired temperature close to the steam cracking temperature without undergoing cracking itself, the mixture passed through Mixer 1 and Mixer II in series. Consequently, the temperature at the outlet of the convection section (Mixer II) was selected to approximate the crossover temperature (XOT) observed in real steam crackers. The feed was then transferred to the topside of the reactor via a high-temperature transfer line (HTTL).

As discussed in section 2.1.3, the temperature profile for the reaction was controlled by adjusting the temperature of three zones. Within this study, two temperature profiles were designated for two different types of experiments. In the instance of profile for high temperature experiment (HT experiments), a temperature elevation of 20°C was applied across all three radiant sections. Throughout the experiments, the first, second, and third reaction zones were maintained at temperatures of 600°C (620°C for HT), 660°C (680°C for HT), and 950°C (970°C for HT) respectively. It is important to note that the temperature measured in this study refers to the outer

wall temperature of the tubular reactor. As a result, the temperature of the gas phase inside the reactor is 50°C lower than the outer wall temperature, falling within the industrial range of operational temperatures. [1]. The difference between the wall temperature and gas temperature has been measured in a pre-experimental test using a movable thermocouple inserted inside the reactor tube, similar to the method used by Geerts et al. [3]. The temperature selected for this study was determined with the aim of maintaining the propylene-to-ethylene ratio (P/E) within the range typically observed in industrial practices, which is between 0.4 and 0.5 [34]. This ratio is widely recognized as an indicator of the severity of the reactions. The temperature control of the transfer line exchanger (TLE) section was achieved using a ratio controller that regulated the heating rate of the furnace and the flow rate of cooling air to attain the desired process value. In all experiments, the temperature of the TLE was set to 400°C. Each cracking run lasted for 6 hours at a coil outlet pressure (COP) of 180 kPa (controlled by BPR). Subsequently, the tubular reactor was cooled down and purged to remove any remaining hydrocarbon. Detailed information on the cooling, purging, and reactor decoking procedures can be found in section S4 of the Supporting Information.

Table 3. Overview of operating conditions for different phases of experiments in the FAST. For the HT experiments, a temperature increase of 20°C was implemented across all experimental phases within the three reaction zones.

	Pretreatment			Cracking	Cooling and Purging		
	Step 1	Step 2	Pre Sulfidation		Step 1	Step 2	Step 3
TLE	400 °C	400 °C	400 °C	400 °C	400 °C	400 °C	20 °C
Reaction Zone 3 (Cracking zone)[1]	300-950 °C (50°C/h)	950 °C (for 5 hours)	827 °C (for 30 minutes)	950 °C (for 6 hours)	Reduce temp. to 400 °C N_2: 70g/h	400 °C (for 2 hours) Steam: 35g/h +	Reduce temp. to 20 °C (for 4 hours) N_2: 70g/h
	Steam: 35g/h +	Steam: 35g/h +	DMDS solution (500 wt. ppm):	DMDS solution (60 wt. ppm): 49g/h + HC:140g/h + N_2 (IS): 20g/h			

	N_2:20g /h	N_2:20g /h	35g/h + N_2:20g/h		N_2:70 g/h		
Reaction Zone 2[1]	660 °C		660 °C	660 °C			
Reaction Zone 1[1]	600 °C		600 °C	600 °C			
Mixer II[2]	400 °C		400 °C	400 °C			
Mixer I[2]	260 °C		260 °C	260 °C	260 °C	260 °C	20 °C
SG[2]	200 °C Steam		200 °C Steam	200 °C Steam	200 °C	200 °C Steam	20 °C
DFP[2]	150 °C N_2		150 °C N_2	150 °C Liquid HC	150 °C N_2	150 °C N_2	150 °C N_2

[1]Set temperature = wall temperature; [2]Set temperature = process gas temperature

In this study, the experimental trends were analyzed based on a one-way analysis of variance (ANOVA) to test the significance of the observed trends. A p-test was performed to assess the difference between the groups. The p-values were computed via Python utilizing the Statsmodels package [35]. A p-value < 0.05 was deemed to be statistically significant throughout this work.

3. Results and Discussion

3.1. Effect of feedstock composition on fouling

The assessment of fouling in the radiant section was conducted online through gravimetrical measurements. In the online method, the mass of coke deposited on a coupon placed in the radiant section was continuously monitored using the Magnetic Suspension Balance (MSB).

Figure 3 illustrates an example of filtered coking and derived fitted coking curve, as well as the corresponding coking rate curve obtained by differentiating the fitted coking curve in the A1 experiment. The catalytic and asymptotic coking rates derived from the coking rate curves of different feedstocks are depicted in Figure 4. The error bars' magnitude represents one standard

deviation on both sides. The intervals of 45 minutes to 1 hour and 5 to 6 hours were identified as the catalytic and asymptotic fouling regimes, respectively.

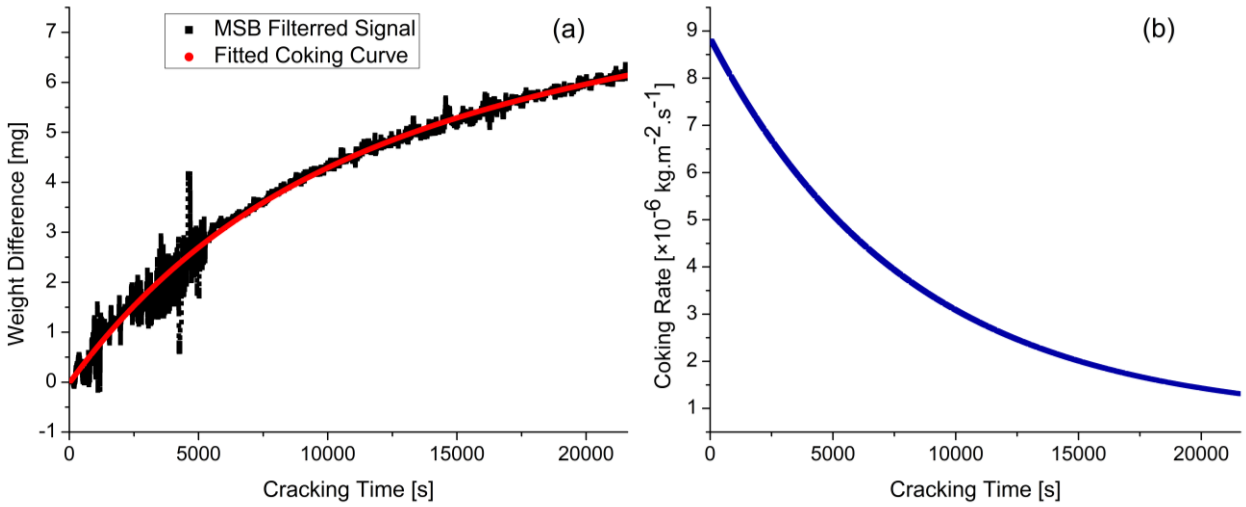

Figure 3. (a): filtered and fitted coking curve for an experiment with A1 sample at COT=950°C; (b): correspond coking rate obtaining by differentiating the fitted coking curve.

The catalytic coking rate primarily depends on the surface properties and the activity of catalytic sites such as Ni and Fe during the initial stages of the reaction [7, 10, 33, 36]. Various factors, such as the roughness and oxide layer integrity of the coupon material, which are dependent on the manufacturing of the coupons, influence this phenomenon. Additionally, fluctuations in temperature (due to the endothermic nature of the reaction [10]) and pressure at the beginning of the experiment affect the measured catalytic coking rates. These factors impact the measurement of the catalytic coking rate and result in less accuracy compared to the asymptotic coking rate. Geerts et al. [3] reported approximately 14% uncertainty in calculating the catalytic coking rate using the same apparatus. This was further confirmed by a one-way ANOVA, resulting in a p-value of 0.61, indicating that the effect of dopants and temperature is statistically insignificant for catalytic coking rate. The catalytic coking rates in this study fall within an average range between 3.89 and

4.77 ($\times 10^{-6}$ kg.m^{-2}.s^{-1}). On the other hand, the asymptotic coking rate, which is deemed to be the most significant parameter for assessing fouling tendencies in the radiant section and playing a crucial role in industrial steam cracking processes, predominantly relates to the feedstock composition [14]. Analysis of Figure 4 reveals that the inclusion of single-ring aromatics i.e., benzene and toluene up to 9 wt.% led to a negligible 6% reduction in the asymptotic coking rate. However, an increase in naphthalene and acenaphthylene resulted in 9% and 42% higher asymptotic coking rates, respectively. This can be attributed to the high fouling tendency of polycyclic aromatic hydrocarbons (PAH), like naphthalene and acenaphthylene in the cracking environment. These compounds can undergo dehydrogenation, abstract radicals in the gas phase, and increase their aromatic ring numbers, ultimately leading to coke deposition on the coupon [22, 24, 37]. Especially acenaphthylene has a significant impact on the coking rate with a p-value of 0.037. The importance of these values is underscored in the research conducted by Van Geem et al. [38], which demonstrated that a 10% reduction in the coking rate can extend the steam cracker run length by approximately 15 days.

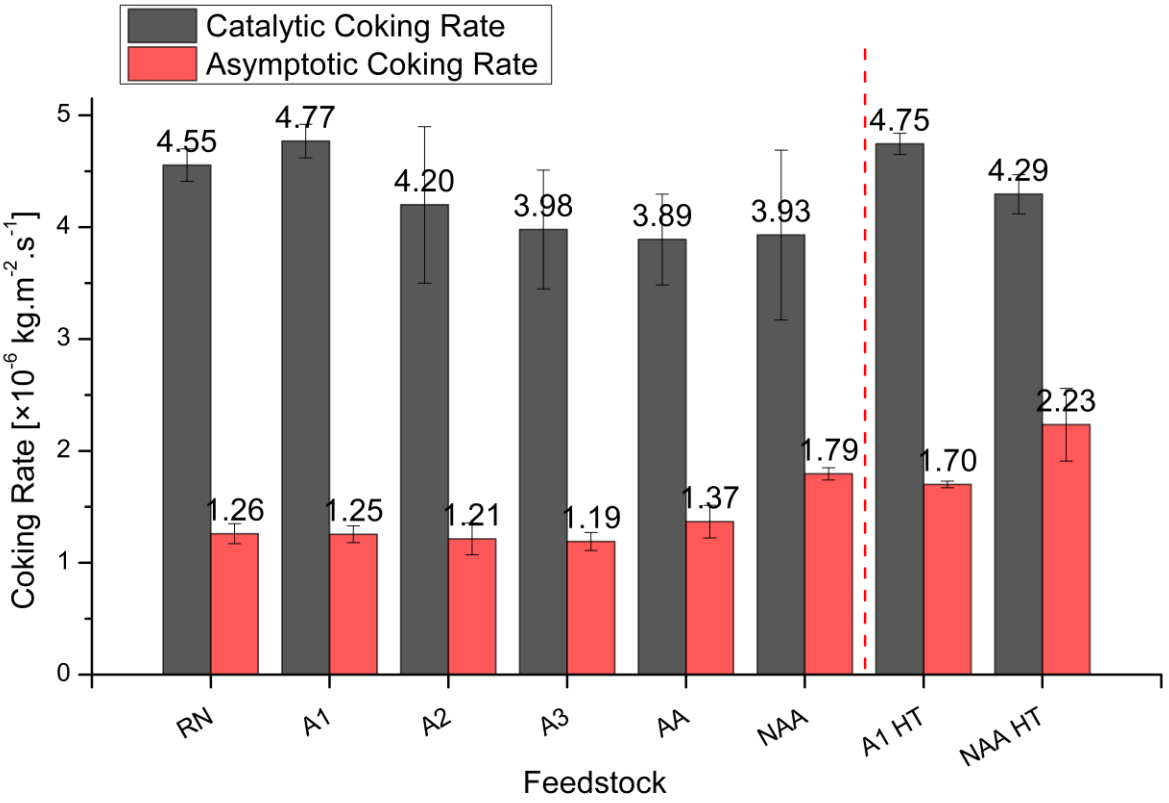

Figure 4. Catalytic and asymptotic coking rates obtained from online coke measurements in steam cracking with feedstocks: RN, A1, A2, A3, AA, and NAA. HT denotes 20℃ higher cracking temperature. The error bars' magnitude represents a standard deviation on both sides.

Table 4 presents a summary of the compositional analysis of the reactor effluent obtained from various feedstocks and experimental conditions using RGA and GC×GC. A comprehensive analysis of the product compositions can be found in section S6 of the Supporting Information. According to this analysis and based on the experimental conditions, the residence time in the radiant and TLE sections was calculated to be 0.41 and 0.16 s, respectively. Also, Figure S.3 in section S5 of the Supporting Information shows a 2D chromatogram of the NAA feedstock. Since all components shown in this chromatogram are also present in all cracking effluents, it showcases a typical 2D gas chromatogram for all cracked effluents in this study. Additionally, the quantification of coke deposits in the radiant and TLE sections was performed through the post-cracking decoking procedure. The average fouling rate in each section was determined by dividing

the total amount of coke deposits by the duration of the six-hour cracking experiment, as depicted in Figure 5. The size of the error bars represents one standard deviation in both sides.

Table 4. Summary of the compositional analysis of the steam cracking products at COT=950°C and COT=970°C (HT) with different feedstocks.

Components [wt.%]	RN	A1	A2	A3	AA	NAA	A1 HT	NAA HT
Total C4-	62.03	62.22	61.07	59.23	63.12	61.17	64.33	63.35
Total C5+	35.67	35.77	38.93	40.77	36.88	38.82	35.67	36.65
Propylene/Ethylene	0.47	0.47	0.45	0.43	0.47	0.47	0.36	0.37
C2H4	24.22	24.11	23.44	23.20	23.87	23.20	26.38	26.59
C3H6	11.44	11.22	10.65	9.95	11.30	10.94	9.45	9.89
Benzene	6.38	6.88	7.21	9.57	5.92	6.53	10.13	9.00
Toluene	2.31	2.50	3.37	4.50	1.99	2.28	2.75	2.36
Xylenes	0.62	0.67	0.56	0.59	0.62	0.59	0.83	0.79
Styrene	0.35	0.30	0.29	0.47	0.20	0.25	0.66	0.52
Methyl Styrene	0.12	0.11	0.10	0.15	0.09	0.10	0.15	0.13
Indene	0.20	0.19	0.19	0.26	0.19	0.20	0.40	0.38
Naphthalene	0.58	0.61	0.63	0.89	2.18	1.18	1.54	1.24
Acenaphthylene	0.06	0.07	0.06	0.06	0.15	0.50	0.32	1.15
Naphthene-aromatics	0.17	0.17	0.16	0.19	0.13	0.18	0.29	0.24
Diaromatics	1.09	1.14	1.23	1.16	2.43	1.05	2.27	2.06
Naphthene di-aromatics	0.10	0.09	0.13	0.11	0.20	0.78	0.58	1.70
Triaromatics	0.00	0.00	0.00	0.00	0.00	0.00	0.25	0.46
PFO (C10+)	1.42	1.41	1.52	1.45	2.75	2.01	3.38	4.47
PAH	1.21	1.23	1.36	1.27	2.63	1.83	3.10	4.22

Based on the offline coking measurements, it can be concluded that the inclusion of benzene and toluene as spiking components did not lead to increased fouling in the TLE section. However, as the number of aromatic rings increases, a higher level of fouling in the TLE section can be observed. In comparison to the RN sample, NAA samples resulted in 14% more coke deposition rate, respectively (p-value of 0.06). This increase in fouling is associated with higher yields of pyrolysis fuel oil (PFO), indicating that the condensation of heavy hydrocarbons serves as the

primary fouling mechanism in the TLE section [39]. Although the AA exhibits higher levels of PFO and PAH compared to the NAA, it generates less coke in the TLE section. This is attributed to the greater coke-forming activity of acenaphthylene relative to naphthalene, which is more abundant in the steam cracking effluent of the NAA sample. Furthermore, when examining the compositional analysis of the steam cracking products from these two samples, it can be inferred that a substantial portion of the naphthalene injected into the RN sample is detected in the steam cracking products of AA. In contrast, only 0.42% of the acenaphthylene in the NAA sample is detected in the products of the NAA sample. This points to the high reactivity of acenaphthylene, contributing to secondary reactions and resulting in the formation of coke. Additional experiments utilizing MSB measurements in the TLE could offer further insights.

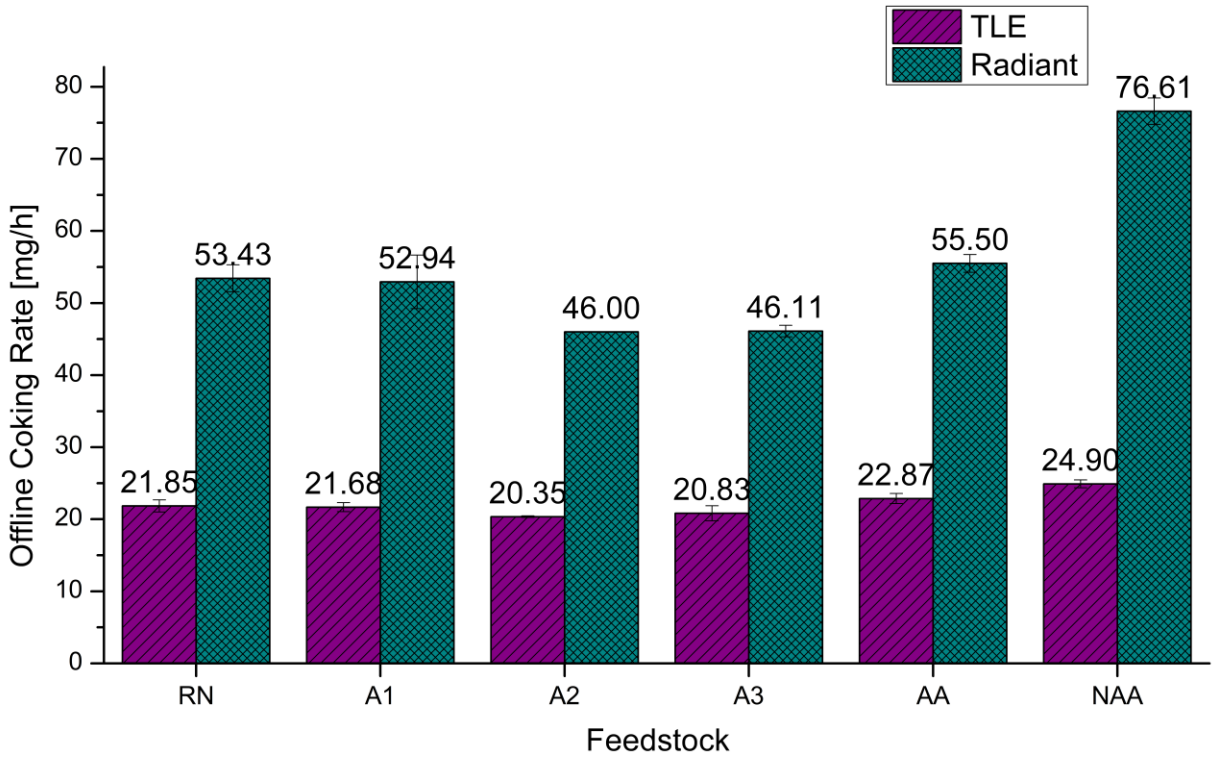

Figure 5. Coking rates obtained from offline decoking (IR) associated with different feedstocks subjected to steam cracking at COT 950°C. The size of the error bars represents one standard deviation on both sides.

The measurement of the overall amount of coke in the radiant section deposited over the complete experimental run provides additional insight into the differences in coking tendencies among various feedstocks and the impact of specific aromatic components. In the radiant section, the addition of single-ring aromatics led to a decrease in coke formation. This is consistent with the findings from the online coke measurements. For instance, the A3 sample generated 14% less coke compared to the RN sample. This can be attributed to the higher production of olefins during the cracking of the RN sample, which are precursors for coke formation in the radiant section [5, 17]. This higher production of olefins is a result of the elevated presence of paraffins and iso-paraffins in the feedstock with lower aromatic content. Another contributing factor is the presence of benzene and toluene, which have limited reactivity in the radiant section and do not actively participate in coke formation reactions. This observation aligns with the findings of Kopinke et al., who conducted experiments with tracer isotope components spiked into a naphtha sample and found that the addition of benzene and toluene has a positive effect on reducing coke formation [22]. Tesner et al. [39, 40]and Magaril et al. [41] also determined relative coking rate constants of 0.36 for benzene compared to naphtha in the radiant section. It is important to note that the single-ring aromatics examined in this study encompass aromatics with a single ring, either with or without only one methyl chain substituent group. It is anticipated that by increasing the number and length of the substituent alkyl groups linked to the aromatic rings, there will be an increase in the tendency for coking. [22]. Similar to the TLE, the trend of increasing coke formation rate is observed when transitioning from single-ring aromatics to double-ring aromatic and naphtheno-diaromatic in the radiant section. This trend is particularly pronounced in the case of the NAA sample, where the coking rate is 43% higher than that of the RN sample. This aligns with the results observed in the online coke measurements, indicating a 42% rise in the asymptotic coking rate when the RN was

spiked with acenaphthylene. This can be attributed to the acenaphthylene's high reactivity within the cracking environment and its strong propensity for coke formation. This is evident from the fact that most of the acenaphthylene present in the feedstock remains in the reactor, with only a small amount being detected in the effluent through GC×GC analysis (Table 4).

To compare the coking rates of the feedstocks studied in this research with those which can be derived from the work of Kopinke et al. [5, 21, 22] in the radiant section, a dimensionless number R_i is introduced, which is a measure of the relative difference in coking rates of a specific sample compared to reference naphtha (RN). This parameter R_i is defined by Eq. (6):

$$R_i = 100\left(\frac{r_f - r_{RN}}{r_{RN}}\right) \qquad \text{Eq. (6)}$$

In Eq. (6), r_{RN} represents the coking rate of the RN sample obtained in our experimental study, while r_f represents the coking rates of the feedstocks obtained from both our study and coking rates $r_{f,KP}$ calculated based on the relative coking rate constants from Kopinke's research, in conjunction with the weight percentages of the added compounds (Eq. (7)).

$$r_{f,KP} = y_{RN}r_{RN} + (y_B - 0.0063)r_B + (y_T - 0.0085)r_T + (y_N r_N) + (y_A r_A) \qquad \text{Eq. (7)}$$

in which B, T, N, and A refer to benzene, toluene, naphthalene, and acenaphthylene, respectively. In Eq. (7), $r_{f,KP}$ represents the calculated coking rate of a specific feedstock based on Kopinke's specific relative coking rate constants r_B, r_T, r_N and r_A for benzene, toluene, naphthalene, and acenaphthylene, respectively, y_{RN} is the weight percentage of reference naphtha in the feedstock, y represents the weight percentage of a particular component in the feedstock. The values 0.0063 and 0.0085 represent the weight percentages of benzene and toluene in the studied reference

naphtha. Kopinke's methodology yielded relative coking rates of $r_B = 0.30$, , $r_T = 0.62$, $r_N = 0.95$, and $r_A = 5.9$ in the radiant section, and $r_B = 0.325$, $r_T = 1.1$, $r_N = 2.4$, and $r_A = 30$ in the TLE section.

Figure 6 demonstrates the relative coking rate difference R_i for different studied feedstocks. By examining Figure 6, it can be inferred that in Kopinke's work, the addition of single-ring aromatics up to 9 wt.% resulted in a maximum reduction of coke formation by 1.78% and 3.90% in the TLE and radiant sections, respectively. These values were more pronounced in the FAST unit due to the higher temperature (COT 950°C) employed in contrast to the lower temperature of 810°C in Kopinke's study. This was also the case for naphthalene, as its addition led to higher fouling in both the radiant and TLE sections, resulting in 3.88% and 4.67% higher coking rates in the radiant and TLE sections, respectively. Notably, the variation in coking between this study and Kopinke's is evident in the experiment with the NAA sample. In Kopinke's work, a higher rate of coke formation was observed in the TLE section compared to this study, which can be attributed to the different temperature profiles in which the TLE section reached temperatures up to 200°C, facilitating the condensation of heavy polynuclear aromatics on the wall or in the bulk gas phase, subsequently collecting on the wall [8, 9, 13, 17, 18, 23, 42-47]. Conversely, in the radiant section, a significantly higher amount of coke was formed in this study compared to the value calculated using Kopinke's rate constants. This difference can be attributed to the more intense cracking conditions in this study, enhancing the reactivity of acenaphthylene. These results emphasize the significant influence of increasing temperature on facilitating secondary reactions that contribute to coke formation in the radiant section. Furthermore, it confirms that lowering the temperature in the TLE section intensifies the condensation mechanism, leading to increased coke deposition. Overall, the fouling results obtained are consistent with the simple fouling model derived from the work of Kopinke et al. Any discrepancies between the model and experimental results should be

attributed to variations in feedstocks, experimental units, methods of fouling assessment, and particularly experimental temperature conditions in the radiant and TLE sections.

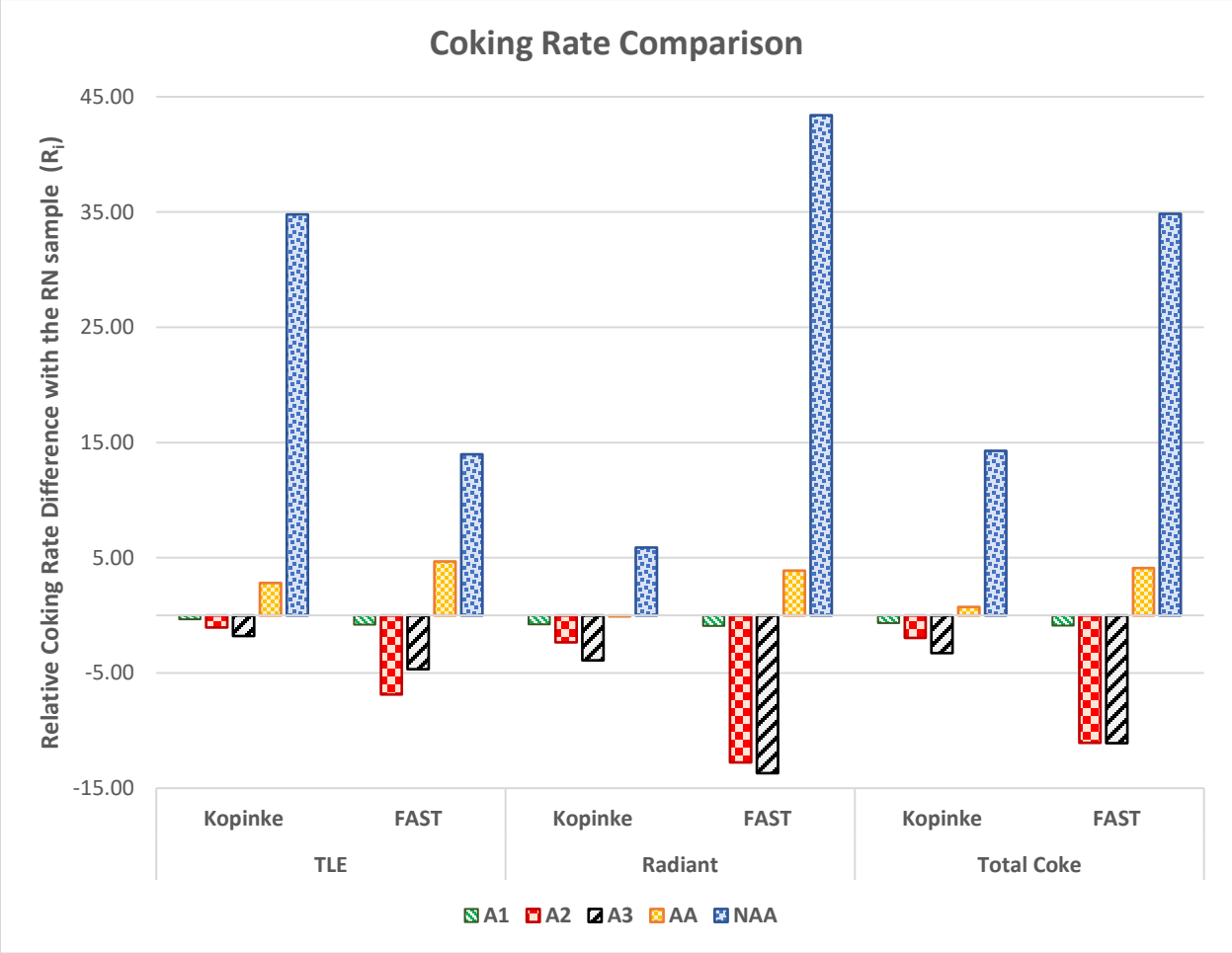

Figure 6. Comparative analysis of coking rate data between the present study and those obtained by calculating from Kopinke et al.'s relative coking rates [22].

In addition to the relative coking rate difference with the RN sample, the relative coking rate constants for the aromatics, defined as their relative coking rate tendency compared to the reference naphtha, were calculated using Eq. (7). These are provided in Table S.7 in the Supporting Information.

3.2. Temperature vs. Feedstock: Effects on fouling

Investigating the impact of temperature and its relative significance when compared to feedstock effects on coke formation was another goal of this study. The experimental configuration involved utilizing two different samples, namely A1 and NAA. Both samples underwent the steam cracking process at an elevated temperature of 970°C i.e., a temperature rise of 20°C, and each test was duplicated. Through a comparison of online coke measurements during the cracking of A1 and NAA at two different temperatures (as shown in Figure 4), it became evident that the catalytic rates obtained were remarkably similar. As detailed in section 3.1, the catalytic rate is predominantly influenced by surface properties. Activation energies for the catalytic reactions are also lower as compared with those of the radical reactions and, hence, the effect of temperature on the catalytic coking is expected to be less than for the asymptotic coking rates [48]. Nevertheless, the asymptotic coking rate, a critical factor in determining the duration of a steam cracker operation [14], was primarily influenced by temperature. In the case of the A1 and NAA samples, as depicted in Figure 4, the asymptotic coking rate displayed an average significant increase of 36% and 25%, respectively, at the higher temperature. This highlights the substantial impact of even a slight temperature rise of 20°C on coking tendencies.

When comparing coking rates obtained from offline coke measurements (as presented in Table S8 in section S8 of the Supporting Information and shown in Figure 7, it becomes evident that temperature elevation had a significant effect on the formation of coke in the TLE section. The deposition of coke notably increased by 71% and 97% for the A1 and NAA feeds, respectively, due to the 20°C temperature rise (p-values of 0.005 and 0.003 respectively). This phenomenon is closely tied to the mechanism of fouling in the TLE section, primarily driven by a condensation mechanism, in which high-boiling-point compounds present in the reactor effluent act as

precursors for coke formation [21, 22, 49]. This mechanism is linked to a respective increase of 2.4 and 2.2 times in the concentrations of pyrolysis fuel oil (PFO) and 2.5 and 2.3 times in polycyclic aromatic hydrocarbons (PAH) for the A1 and NAA feeds, respectively. The heightened presence of PFO and PAH at higher temperatures leads to an increase in condensation and subsequent dehydrogenation reactions, thereby contributing to enhanced coke formation in the TLE section [3, 24, 49, 50]. At the elevated temperature of 970 °C, the effect of doping is even more pronounced than at the original temperature of 950 °C. While at 950 °C the increase in coking by doping with acenaphthylene is only 15% compared to A1, this increases to 32% for NAA compared to A1 at 970 °C.

As shown in Figure 7, in the radiant section, a parallel trend has been consistently observed. Both the A1 and NAA samples exhibited a significant increase in coke formation of 24% and 22%, respectively, when subjected to elevated temperatures. This phenomenon can be attributed to the heightened activity of coke precursors at elevated temperatures, facilitating higher coke production. When the cumulative coking of TLE and radiant sections are considered, the results highlight a substantial increase in coke formation for both the A1 and NAA samples, amounting to 38% and 40% respectively.

In Figure 7, when examining the offline coking results of the A1 sample at a higher temperature (970°C), it yielded 102.77 mg/h of coke (considering both TLE and radiant). Comparing this with the NAA sample at a lower temperature (950°C), which produced 101.52 mg/h, it is clear that a 20°C temperature increase had a similar effect on coke formation as introducing 1.2 wt.% of naphtheno-diaromatic compounds into naphtha. This underscores how even a mere 20°C temperature rise or decrease can significantly impact coke production. Furthermore, it points

toward the potential to efficiently utilize heavier feedstocks containing higher levels of aromatic compounds, by employing a meticulously optimized temperature profile in steam crackers.

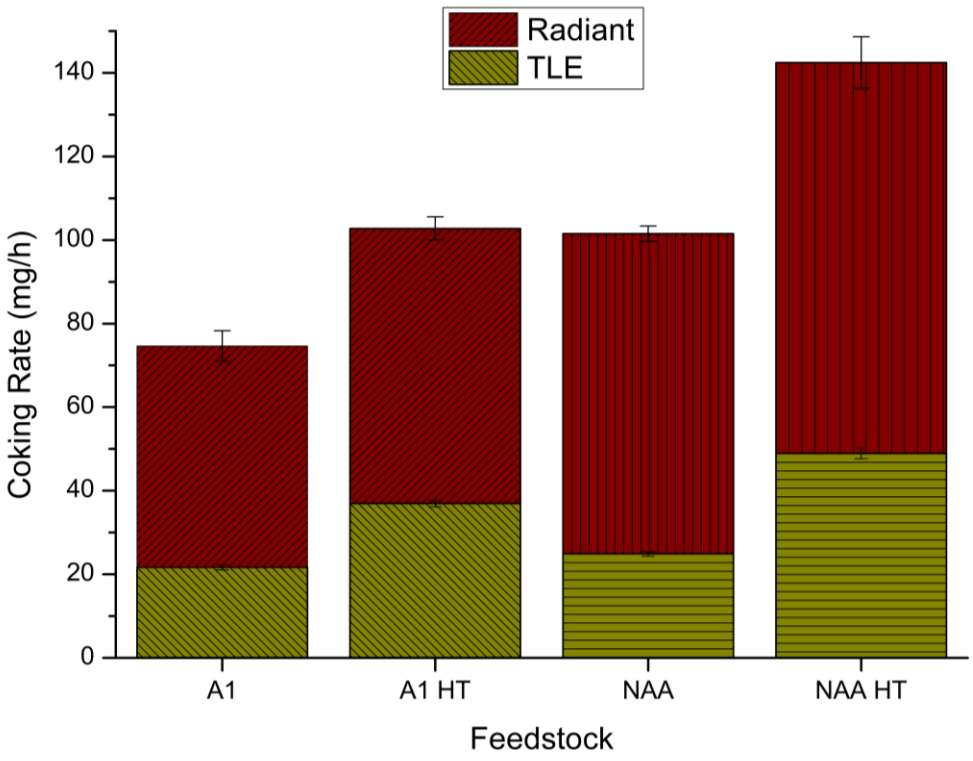

Figure 7. Coking rate comparison of two samples of A1 and NAA at two steam cracking temperatures of 950°C and 970°C. The size of the error bars represents one standard deviation on both sides.

4. Conclusion

In summary, this study employed the Fouling Assessment SetUp (FAST) to comprehensively investigate the influence of feedstock aromaticity and temperature on fouling within the radiant and TLE sections of steam crackers. The utilization of both online and offline coke measurements facilitated a thorough examination of catalytic and asymptotic coking rates, providing valuable insights into the factors affecting the steam cracking run length.

Analysis of various feedstocks revealed noteworthy findings regarding the asymptotic coking rate, a critical parameter in operational duration determination. Increasing single-ring aromatics up to 9 wt.% resulted in a 6% decrease in asymptotic coking rates, while the introduction of double-ring aromatics (2 wt.%) and naphtheno-diaromatics (1.2 wt.%) led to 9% and 42% higher asymptotic rates, respectively. This elevation was attributed to the increased activity of these compounds as coke precursors. Offline coke measurements on the reactor inner wall validated these results, demonstrating a 43% increase in the radiant section's coking rate upon adding 1.2 wt.% acenaphthylene to the naphtha sample. Further investigations into aromatic hydrocarbons with longer alkyl chains are recommended for future research.

In the TLE section, the addition of single-ring aromatics had a minimal impact on fouling, while the introduction of naphthalene and acenaphthylene to naphtha resulted in 5% and 14% higher fouling rates, respectively. This increased fouling tendency was linked to the higher yields of polyaromatic hydrocarbons (PAHs) in the steam cracking products. Consistent results were observed when compared with previous research, with discrepancies attributed to variations in temperature profiles used in the steam cracking reactions.

Elevating the radiant section temperature by 20°C resulted in a minimum 36% increase in asymptotic coking rate, highlighting the significant impact of temperature on coking tendencies. This effect was more pronounced in the TLE section, indicating 2.4 and 2.2 times increases in pyrolysis fuel oil (PFO) concentrations for the A1 and NAA feeds, respectively. The condensation of high-boiling point compounds within the TLE section underscored the substantial influence of even a slight 20°C temperature elevation on fouling. In conclusion, the findings suggest that temperature elevation has a more pronounced effect on fouling in the radiant and TLE sections compared to the introduction of aromatic compounds at the investigated concentrations.

AUTHOR INFORMATION

Corresponding Author

*Kevin M. Van Geem

Laboratory for Chemical Technology, Ghent University, Technologiepark 121, B-9052 Gent, Belgium.. Email: Kevin.VanGeem@UGent.be

Authors

Hamed Mohamadzadeh Shirazi

Laboratory for Chemical Technology, Ghent University, Technologiepark 121, B-9052 Gent, Belgium. Email: Hamed.Mohamadzadeh@UGent.be

Lucas dos Santos Vargette

Laboratory for Chemical Technology, Ghent University, Technologiepark 121, B-9052 Gent, Belgium. Email: Lucas.dossantosvargette@UGent.be

Georgios Bellos

Dow Benelux B.V., Dowweg 5, 4542NM Hoek, The Netherlands. Email: bellos@dow.com

Yannick Ureel

Laboratory for Chemical Technology, Ghent University, Technologiepark 121, B-9052 Gent, Belgium. Email: yannick.ureel@ugent.be

Melissa N. Dunkle

Dow Benelux B.V., Dowweg 5, 4542NM Hoek, The Netherlands. Email: mndunkle@dow.com

Steven Corthals

Dow Benelux B.V., Dowweg 5, 4542NM Hoek, The Netherlands. slcorthals@dow.com

Marie-Françoise Reyniers

Laboratory for Chemical Technology, Ghent University, Technologiepark 121, B-9052 Gent, Belgium. Email: MarieFrancoise.Reyniers@UGent.be

AUTHOR CONTRIBUTIONS

Conceptualization and visualization: Hamed Mohamadzadeh Shirazi, Lucas Dos Santos Vargette, Georgios Bellos, and Kevin M. Van Geem; Data curation and formal analysis: Hamed Mohamadzadeh Shirazi and Lucas Dos Santos Vargette; Investigation and validation: Hamed Mohamadzadeh Shirazi, Georgios Bellos, Kevin M. Van Geem; Methodology: Hamed Mohamadzadeh Shirazi, Lucas Dos Santos Vargette, Georgios Bellos and Kevin M. Van Geem; Funding acquisition, project administration, resources and supervision: Marie-Françoise Reyniers, Kevin M. Van Geem, and Georgios Bellos; Software: Hamed Mohamadzadeh Shirazi and Yannick Ureel; Writing – original draft: Hamed Mohamadzadeh Shirazi; Writing – review & editing: Hamed Mohamadzadeh Shirazi, Lucas Dos Santos Vargette, Georgios Bellos, Melissa N. Dunkle, Steven Corthals, Marie-Françoise Reyniers and Kevin M. Van Geem.

DECLARATION OF COMPETING INTERESTS

The authors declare that they have no known competing financial interests or personal relationships that could have appeared to influence the work reported in this paper.

ACKNOWLEDGMENT

The authors would like to express their gratitude for the financial support received from the Catalisti SBO project WATCH HBC.2019.0001. Additionally, Kevin M. Van Geem holds the European Research Council (ERC) grant "Process intensification and Innovation in Olefin Production by Multiscale Analysis and design" (OPTIMA), funded by the EU Horizon 2020 program, with the grant agreement ID 818607.

NOMENCLATURE

Roman symbols

A,B,C,D	Parameters in coking curve fitting	-
C_x	Hydrocarbons with x carbon atoms	-
COT	Coil outlet temperature	°C
COP	Coil outlet pressure	Pa
MM_c	Molar mass of carbon	g/mol
m_t	Mass of coke at time x	kg
p_i	Pressure at time i	Pa
$\dot{Q}_t$	Volumetric flowrate	m^3/s
R_c	Rate of mass deposition	kg/s
R	Gas constant	J/mol/K
r_f	Average fouling rate in a specific zone	kg/s
r_f	Rate of mass deposition per surface area	$kg/s/m^2$
S_c	Surface area of coupon	m^2
t	Time	s
T	Temperature	°C
t_c	Duration of cracking experiment	s
$y_{x,i}$	Volumetric concentration of component x at time i	-

Acronyms

A1	Reference naphtha sample spiked with single-ring aromatic (3 wt.%)
A2	Reference naphtha sample spiked with single-ring aromatic (6 wt.%)
A3	Reference naphtha sample spiked with single-ring aromatic (9 wt.%)
AA	Reference naphtha sample spiked with double-ring aromatic (2 wt.%)
NAA	Reference naphtha sample spiked with naphtheno-diaromatic (1.2 wt.%)
A1 HT	Reference naphtha sample spiked with single-ring aromatic (3 wt.%) undergoing high temperature steam cracking
NAA HT	Reference naphtha sample spiked with naphtheno-diaromatic (1.2 wt.%) undergoing high temperature steam cracking
BPR	Back pressure regulator
BTX	Benzene, Toluene & Xylene
DFP	Dry feed preheater
FAST	Fouling assessment setup
FID	Flame ionization detector
GC×GC	2-dimensional gas chromatograph
HTTL	high-temperature transfer line
MSB	Magnetic suspension balance
PAH	Polycyclic aromatic hydrocarbon
PFO	Pyrolysis fuel oil
PIONA	Paraffins, isoparaffins, olefins, naphthenes, aromatics
PLC	Programmable logical controller
Pygas	Pyrolysis gasoline
RGA	Refinery gas analyzer

RN	Reference naphtha sample
SG	Steam generator
TCD	Thermal conductivity detector
TLE	Transfer line exchanger
XOT	Crossover temperature

Sub- and superscripts

t_x	Time x
i	Index of sample points during decoking

Supporting Information: calculation of coking rate, RGA and GC×GC settings, GC×GC chromatogram of feedstock and steam cracking product, steam cracking product analysis, coking rates at different temperatures

References

(1) Zimmermann, H.; Walzl, R. Ethylene. *Ullmann's Encyclopedia of Industrial Chemistry* **2009**. DOI: doi:10.1002/14356007.a10_045.pub3.
(2) Pyl, S. P.; Schietekat, C. M.; Reyniers, M.-F.; Abhari, R.; Marin, G. B.; Van Geem, K. M. Biomass to olefins: Cracking of renewable naphtha. *Chemical engineering journal* **2011**, *176*, 178-187.
(3) Geerts, M.; Ristic, N.; Djokic, M.; Ukkandath Aravindakshan, S.; Marin, G. B.; Van Geem, K. M. Crude to olefins: effect of feedstock composition on coke formation in a bench-scale steam cracking furnace. *Industrial & Engineering Chemistry Research* **2020**, *59* (7), 2849-2859. DOI: https://doi.org/10.1021/acs.iecr.9b06702.
(4) Lederer, J.; Ohanka, V.; Fulin, P.; Sebor, G.; Blazek, J. A study of industrial pyrolysis of the high-bouling products from hydrocracking of petroleum vacuum distillate. *Fuel* **1994**, *73* (2), 295-299. DOI: 10.1016/0016-2361(94)90128-7.
(5) Kopinke, F. D.; Zimmermann, G.; Nowak, S. On the mechanism of coke formation in steam cracking—conclusions from results obtained by tracer experiments. *Carbon* **1988**, *26* (2), 117-124. DOI: https://doi.org/10.1016/0008-6223(88)90027-9.
(6) Mohamadzadeh Shirazi, H.; dos Santos Vargette, L.; Reyniers, M.-F. o.; Van Geem, K. M. Effect of Reactor Alloy Composition on Coke Formation during Butane and Ethane Steam Cracking. *Industrial & Engineering Chemistry Research* **2024**, *63* (5), 2100-2112. DOI: https://doi.org/10.1021/acs.iecr.3c03180.
(7) Mohamadzadeh Shirazi, H.; Ghanbari, A.; Vermeire, F.; Reyniers, M.-F.; Van Geem, K. M. Carburization of High-Temperature Alloys during Steam Cracking: The Impact of Alloy Composition and Temperature. *Industrial & Engineering Chemistry Research* **2023**. DOI: 10.1021/acs.iecr.2c03599.
(8) Wauters, S.; Marin, G. Computer generation of a network of elementary steps for coke formation during the thermal cracking of hydrocarbons. *Chemical Engineering Journal* **2001**, *82* (1-3), 267-279.
(9) Wauters, S.; Marin, G. Kinetic modeling of coke formation during steam cracking. *Industrial & engineering chemistry research* **2002**, *41* (10), 2379-2391.
(10) Muñoz Gandarillas, A. s. E.; Van Geem, K. M.; Reyniers, M.-F. o.; Marin, G. B. Influence of the reactor material composition on coke formation during ethane steam cracking. *Industrial & Engineering Chemistry Research* **2014**, *53* (15), 6358-6371.
(11) Sarris, S. A.; Olahova, N.; Verbeken, K.; Reyniers, M.-F. o.; Marin, G. B.; Van Geem, K. M. Optimization of the in situ pretreatment of high temperature Ni–Cr alloys for ethane steam cracking. *Industrial & Engineering Chemistry Research* **2017**, *56* (6), 1424-1438.

(12) Froment, G. Coke formation in the thermal cracking of hydrocarbons. *Rev. Chem. Eng.* **1990**, *6*, 293-328.
(13) Towfighi, J.; Sadrameli, M.; Niaei, A. Coke formation mechanisms and coke inhibiting methods in pyrolysis furnaces. *Journal of chemical engineering of Japan* **2002**, *35* (10), 923-937.
(14) Reyniers, M.-F. S.; Froment, G. F. Influence of metal surface and sulfur addition on coke deposition in the thermal cracking of hydrocarbons. *Industrial & engineering chemistry research* **1995**, *34* (3), 773-785.
(15) Snoeck, J.-W.; Froment, G.; Fowles, M. Filamentous carbon formation and gasification: thermodynamics, driving force, nucleation, and steady-state growth. *Journal of Catalysis* **1997**, *169* (1), 240-249.
(16) Baker, R.; Yates, D.; Dumesic, J. Filamentous carbon formation over iron surfaces. ACS Publications, 1982; pp 1-21.
(17) Cai, H.; Krzywicki, A.; Oballa, M. C. Coke formation in steam crackers for ethylene production. *Chemical Engineering and Processing: Process Intensification* **2002**, *41* (3), 199-214.
(18) Wang, J.; Reyniers, M.-F.; Marin, G. B. The influence of phosphorus containing compounds on steam cracking of n-hexane. *Journal of analytical and applied pyrolysis* **2006**, *77* (2), 133-148.
(19) Ranzi, E.; Dente, M.; Pierucci, S.; Barendregt, S.; Cronin, P. Coking simulation aids on-stream time. *Oil & gas journal* **1985**, *83* (35), 49-52.
(20) Gál, T.; Lakatos, B. G. Thermal cracking of recycled hydrocarbon gas-mixtures for re-pyrolysis: Operational analysis of some industrial furnaces. *Applied Thermal Engineering* **2008**, *28* (2), 218-225. DOI: https://doi.org/10.1016/j.applthermaleng.2007.03.020.
(21) Kopinke, F. D.; Zimmermann, G.; Reyniers, G. C.; Froment, G. F. Relative rates of coke formation from hydrocarbons in steam cracking of naphtha. 2. Paraffins, naphthenes, mono-, di-, and cycloolefins, and acetylenes. *Industrial & Engineering Chemistry Research* **1993**, *32* (1), 56-61. DOI: 10.1021/ie00013a009.
(22) Kopinke, F. D.; Zimmermann, G.; Reyniers, G. C.; Froment, G. F. Relative rates of coke formation from hydrocarbons in steam cracking of naphtha. 3. Aromatic hydrocarbons. *Industrial & Engineering Chemistry Research* **1993**, *32* (11), 2620-2625.
(23) Geem, K. M. V.; Dhuyvetter, I.; Prokopiev, S.; Reyniers, M.-F.; Viennet, D.; Marin, G. B. Coke formation in the transfer line exchanger during steam cracking of hydrocarbons. *Industrial & engineering chemistry research* **2009**, *48* (23), 10343-10358.
(24) Zhang, J.; Van de Vijver, R.; Amghizar, I.; Reyniers, M.-F. o.; Van Geem, K. M. Combined Catalytic and Pyrolytic Coking Model for Steam Cracking of Hydrocarbons. *Industrial & Engineering Chemistry Research* **2022**, *61* (11), 3917-3927.
(25) Zimmermann, G.; Zychlinski, W.; Woerde, H. M.; van den Oosterkamp, P. Absolute rates of coke formation: A relative measure for the assessment of the chemical behavior of high-temperature steels of different sources. *Industrial & engineering chemistry research* **1998**, *37* (11), 4302-4305.
(26) Kopinke, F.-D.; Ondruschka, B.; Zimmermann, G.; Dermietzel, J. Rearrangement reactions in the thermal formation of aromatics from cycloolefins. 14C-labelling studies. *Journal of analytical and applied pyrolysis* **1988**, *13* (4), 259-275.
(27) Van Geem, K. M.; Pyl, S. P.; Reyniers, M.-F.; Vercammen, J.; Beens, J.; Marin, G. B. On-line analysis of complex hydrocarbon mixtures using comprehensive two-dimensional gas chromatography. *Journal of Chromatography A* **2010**, *1217* (43), 6623-6633.
(28) Ristic, N. D.; Djokic, M. R.; Van Geem, K. M.; Marin, G. B. On-line analysis of nitrogen containing compounds in complex hydrocarbon matrixes. *JoVE (Journal of Visualized Experiments)* **2016**, (114), e54236.
(29) Schoenmakers, P. J.; Oomen, J. L.; Blomberg, J.; Genuit, W.; van Velzen, G. Comparison of comprehensive two-dimensional gas chromatography and gas chromatography–mass spectrometry for

the characterization of complex hydrocarbon mixtures. *Journal of Chromatography A* **2000**, *892* (1-2), 29-46.
(30) Matsumoto, M.; Hayakawa, K.; Kitaoka, S.; Matsubara, H.; Takayama, H.; Kagiya, Y.; Sugita, Y. The effect of preoxidation atmosphere on oxidation behavior and thermal cycle life of thermal barrier coatings. *Materials Science and Engineering: A* **2006**, *441* (1-2), 119-125.
(31) Singh, A.; Paulson, S.; Farag, H.; Birss, V.; Thangadurai, V. Role of Presulfidation and H2S Cofeeding on Carbon Formation on SS304 Alloy during the Ethane–Steam Cracking Process at 700° C. *Industrial & Engineering Chemistry Research* **2018**, *57* (4), 1146-1158.
(32) Symoens, S. H.; Olahova, N.; Muñoz Gandarillas, A. s. E.; Karimi, H.; Djokic, M. R.; Reyniers, M.-F. o.; Marin, G. B.; Van Geem, K. M. State-of-the-art of coke formation during steam cracking: Anti-coking surface technologies. *Industrial & Engineering Chemistry Research* **2018**, *57* (48), 16117-16136.
(33) Jakobi, D.; Karduck, P. Behavior of High-Temperature Tube Materials in Sulfur-Containing Steam-Cracking Conditions. In *NACE International Corrosion Conference Proceedings*, 2018; NACE International: pp 1-17.
(34) De Bruycker, R.; Anthonykutty, J. M.; Linnekoski, J.; Harlin, A.; Lehtonen, J.; Van Geem, K. M.; Räsänen, J.; Marin, G. B. Assessing the potential of crude tall oil for the production of green-base chemicals: an experimental and kinetic modeling study. *Industrial & Engineering Chemistry Research* **2014**, *53* (48), 18430-18442.
(35) Seabold, S.; Perktold, J. Statsmodels: Econometric and statistical modeling with python. 2010, Austin, TX: Vol. 57, pp 10-25080.
(36) Sarris, S. A.; Symoens, S. H.; Olahova, N.; Verbeken, K.; Reyniers, M.-F. o.; Marin, G. B.; Van Geem, K. M. Impact of initial surface roughness and aging on coke formation during ethane steam cracking. *Industrial & Engineering Chemistry Research* **2017**, *56* (44), 12495-12507.
(37) Gholami, Z.; Gholami, F.; Tišler, Z.; Vakili, M. A review on the production of light olefins using steam cracking of hydrocarbons. *Energies* **2021**, *14* (23), 8190.
(38) Van Geem, K. M.; Reyniers, M.-F.; Pyl, S.; Marin, G. B.; Zhou, Z. Effect of operating conditions and feedstock composition on run lengths of steam cracking coils. In *AIChE Spring Meeting: Ethylene producers conference*, 2009.
(39) Tesner, P. Kinetics of pyrolytic carbon formation. In *Chemistry & Physics of Carbon*, CRC Press, 2021; pp 65-161.
(40) Tesner, P. A.; Thrower, P. A. Marcel Dekker, 1984.
(41) Magaril, R. Z.; Berezina, S. N. Zhurnal Fizicheskoi Khimii. *Chem Abstr* **1976**, *50* (50), 2282.
(42) Wang, J.; Reyniers, M.-F.; Marin, G. B. Influence of dimethyl disulfide on coke formation during steam cracking of hydrocarbons. *Industrial & engineering chemistry research* **2007**, *46* (12), 4134-4148.
(43) Wang, J.; Reyniers, M.-F.; Van Geem, K. M.; Marin, G. B. Influence of silicon and silicon/sulfur-containing additives on coke formation during steam cracking of hydrocarbons. *Industrial & Engineering Chemistry Research* **2008**, *47* (5), 1468-1482.
(44) Brown, D. Internally finned radiant coils: A valuable tool for improving ethylene plant economics. In *Proceedings of the 6th EMEA Petrochemicals Technology Conference, London, UK*, 2004; pp 23-26.
(45) Albano, J.; Sundaram, K.; Maddock, M. *Application of extended surfaces in pyrolysis coils*; New York, NY; American Institute of Chemical Engineers, 1988.
(46) Schietekat, C. M.; Van Goethem, M. W.; Van Geem, K. M.; Marin, G. B. Swirl flow tube reactor technology: An experimental and computational fluid dynamics study. *Chemical Engineering Journal* **2014**, *238*, 56-65.
(47) Ropital, F.; Broutin, P.; Reyniers, M.-F.; Froment, G. Anticoking coatings for high temperature petrochemical reactors. *Oil & Gas Science and Technology* **1999**, *54* (3), 375-385.

(48) Reyniers, G. C.; Froment, G. F.; Kopinke, F.-D.; Zimmermann, G. Coke formation in the thermal cracking of hydrocarbons. 4. Modeling of coke formation in naphtha cracking. *Industrial & engineering chemistry research* **1994**, *33* (11), 2584-2590.
(49) Kopinke, F. D.; Bach, G.; Zimmermann, G. New results about the mechanism of TLE fouling in steam crackers. *Journal of Analytical and Applied Pyrolysis* **1993**, *27* (1), 45-55. DOI: https://doi.org/10.1016/0165-2370(93)80021-Q.
(50) Abdel-Shafy, H. I.; Mansour, M. S. A review on polycyclic aromatic hydrocarbons: source, environmental impact, effect on human health and remediation. *Egyptian journal of petroleum* **2016**, *25* (1), 107-123.

For Table of Contents Only